3-[4-Phenoxyphenyl]pyrazole (Hpz^{PP}) and 3-[4-butoxyphenyl]pyrazole (Hpz^{bp}) in rhodium chemistry
Crystal structures of 3-[4-phenoxyphenyl]pyrazole, [Rh(μ-pz^{PP})(COD)]$_2$ · $\frac{1}{2}$CH$_2$Cl$_2$ and [Rh(μ-pz^{bp})(COD)]$_2$

M. Cano [a,*], J.V. Heras [a], M. Maeso [a], M. Alvaro [a], R. Fernández [a], E. Pinilla [a],
J.A. Campo [b], A. Monge [c]

[a] *Departamento de Química Inorgánica I, Facultad de Ciencias Químicas, Universidad Complutense, 28040-Madrid, Spain*

[b] *Departamento de Química Inorgánica y Materiales, Facultad de Ciencias Experimentales y Técnicas, Universidad San Pablo-CEU, Urbanización Monteprincipe, 28660-Boadilla del Monte, Madrid, Spain*

[c] *Instituto de Ciencias de los Materiales, sede D, CSIC, Serrano 113, 28006-Madrid, and Laboratorio de Difracción de Rayos-X, Facultad de Ciencias Químicas, Universidad Complutense, 28040-Madrid, Spain*

Abstract

The novel pyrazoles containing 3-[4-phenoxyphenyl] (pp) and 3-[4-butoxyphenyl] (bp) substituents, Hpz^{PP} and Hpz^{bp}, have been synthetized and characterized, and the crystalline structure of 3-[4-phenoxiphenyl]pyrazole (Hpz^{PP}) is also reported.

Rh(I) compounds [Rh(Cl)(Hpz^R)(LL)] and [Rh(μ-pz^R)(LL)]$_2$ (LL = NBD, COD, 2CO; R = pp, bp) have been prepared in order to explore the influence of the alkoxy- or aryloxyphenyl substituents on the pyrazol ring of some features such as the presence of dynamic processes or the preference of determined isomers in the complexes.

The molecular structures of complexes [Rh(Cl)(Hpz^R)(LL)] and [Rh(μ-pz^R)(LL)]$_2$ (LL = NBD, COD, 2CO; R = pp, bp) have been studied by IR and ^{1}H and ^{13}C NMR spectroscopies.

^{1}H NMR spectra of compounds [Rh(Cl)(Hpz^R)(LL)] (LL = NBD, COD, 2CO; R = pp, bp) indicate that the presence of a metallotropic equilibrium only depends on the steric characteristics of the ancillary ligands.

On the other hand, complexes [Rh(μ-pz^R)(CO)$_2$]$_2$ (R = pp, bp) are formed as a mixture of the head-to-head (H-H) and head-to-tail (H-T) configurational isomers. By contrast, [Rh(μ-pz^R)(LL)]$_2$ (LL = NBD, COD; R = pp, bp) have been obtained as only one isomer in both the solid state and the solution. The crystalline structures of complexes [Rh(μ-pz^{PP})(COD)]$_2$ · $\frac{1}{2}$CH$_2$Cl$_2$ and [Rh(μ-pz^{bp})(COD)]$_2$ have been solved, showing the presence of the H-T configurational isomer in both cases.

The ^{1}H NMR spectra of [Rh(μ-pz^R)(LL)]$_2$ (LL = NBD, COD, 2CO; R = pp, bp) show that the *ortho* protons of the C$_6$H$_4$ group of the substituents on the pyrazol ring are considerably deshielded. Furthermore, the X-ray structures of [Rh(μ-pz^{PP})(COD)]$_2$ · $\frac{1}{2}$CH$_2$Cl$_2$ and [Rh(μ-pz^{bp})(COD)]$_2$ complexes show an Rh-H(*ortho*) distance of ca. 2.7 Å, characteristic of a weak preagostic interaction.

Keywords: Bulky substituted-pyrazole ligands; Rhodium–pyrazol complexes; Rhodium–pyrazolate complexes; Metallotropy; Conformational isomerism

1. Introduction

The pyrazole-type ligands are an important group in organometallic chemistry [1] and pyrazolate or pyrazol–metal complexes have attracted substantial interest from the point of view of their catalytic activity [2].

Coordination chemistry of pyrazol ligands has been well established, but there are few data related with the influence of the substituents on the pyrazol ring towards the dynamic and stereochemical properties of the complexes.

Previous work from this laboratory dealt with Rh(I) compounds containing bulky pyrazol ligands substituted in the 3(5) position, and some interesting features have been found depending on the substituent on the pyrazol ring [3,4].

* Corresponding author.

So, for square-plane complexes of the type [Rh(Cl(NBD)(Hpz^R)] (NBD = 2,5-norbornadiene; Hpz^R = Hpz, Hpz^{Me2}, Hpz^{Bu}, Hpz^{Me,Bu}, Hpz^{Ph}, Hpz^{Me,Ph}, Hpz^{An}) a metallotropic equilibrium was found in the case of the less demanding substituted-pyrazol ligands [3].
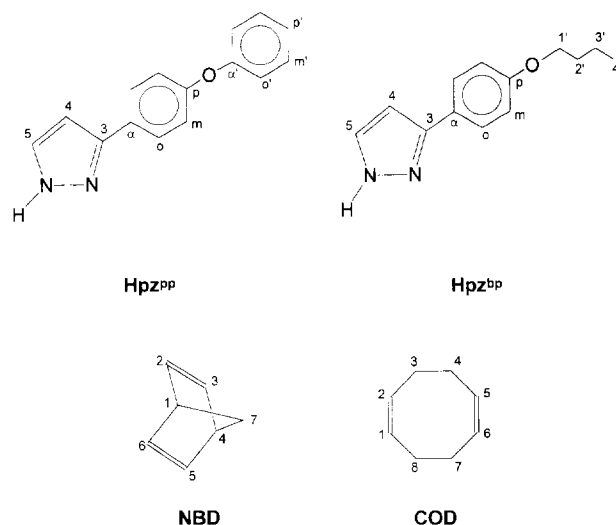
On the other hand, related dinuclear complexes of the type [Rh(μ-pz^R)(LL)]$_2$ (LL = NBD, 2CO; Hpz^R = Hpz, Hpz^{Me2}, Hpz^{Bu}, Hpz^{Me,Bu}, Hpz^{Ph}, Hpz^{Me,Ph}, Hpz^{An}) were isolated as a mixture of the head-to-head (H-H) and head-to-tail (H-T) configurational isomers, or only as one isomer depending on the substituent on the pyrazol ring. It was interesting to note that the complexes containing aryl substituents were always obtained as a mixture of both isomers [4]. A dynamic behaviour in solution at room temperature was observed in some of these complexes and in related olefinic dinuclear derivatives, which was explained in terms of diolefin motions [4,5].

As extension of the above results, in this work, two new substituted-pyrazole ligands, 3-[4-phenoxyphenyl]pyrazole (Hpz^{pp}, 1) and 3-[4-butoxyphenyl]pyrazole (Hpz^{bp}, 2), have been synthetized as well as their corresponding metal derivatives of the type [Rh(Cl)(Hpz^R)(LL)] (3–8) and [Rh(μ-pz^R)(LL)]$_2$ (9–14) (LL = NBD, 1,5-cyclooctadiene (COD), 2CO; R = pp, bp) (Scheme 1). The aim of this work is to explore the effects that changes in the oxyphenyl groups on the pyrazol ligand and in the ancillary ligands would have on the properties of the complexes. The possibility of an Rh–H interaction with the hydrogen atoms in *ortho* position of the C$_6$H$_4$ group of the substituents is also analysed.

2. Experimental section

The reactions were performed at room temperature. Commercial solvents were dried prior to use. Syntheses of the starting Rh-complexes [Rh(μ-Cl)(LL)]$_2$ (LL = NBD, COD) have been described previously [6,7].

Elemental analyses for carbon, hydrogen and nitrogen were carried out by the Microanalytical Service of the Complutense University. IR spectra were recorded on an FTIR Nicolet Magna-550 in KBr discs and, when necessary, in different solvents. ^{1}H NMR spectra were performed on a Varian XL-300 (299.95 MHz) and on a Bruker AM-300 (300.13 MHz) spectrometer. The ^{13}C NMR spectra were recorded on the latter spectrometer working at 75.43 MHz. Chemical shifts δ are listed in parts per million relative to tetramethylsilane; coupling constants J are in hertz. The ^{1}H and ^{13}C chemical shifts are accurate to 0.01 ppm and 0.1 ppm respectively. Coupling constants are accurate to ± 0.3 Hz for ^{1}H NMR spectra and ± 0.6 Hz for ^{13}C NMR spectra.

Hpz^{pp} Hpz^{bp}

NBD   COD

	R	LL	Number
Hpz^R	pp		1
	bp		2
[RhCl(Hpz^R)(LL)]	pp	NBD	3
	pp	COD	4
	bp	NBD	5
	bp	COD	6
	pp	2CO	7
	bp	2CO	8
[Rh(μ-pz^R)(LL)]$_2$	pp	NBD	9
	pp	COD	10
	bp	NBD	11
	bp	COD	12
	pp	2CO	13
	bp	2CO	14

Scheme 1.

2.1. Preparation of Hpz^R (R = pp, bp) (1,2)

A solution of the corresponding substituted acetophenone (9.42 mmol) in ethyl formate (1.16 ml, 14.13 mmol) and toluene (15 ml) was added in a single portion to a slurry of anhydrous sodium methoxide (0.51 g, 9.42 mmol) in toluene (50 ml). A clear solution was obtained, which became a slurry after 5 min. The solid was isolated by filtration after 2 h at room temperature and washed with hexane.

The solid was dissolved in methanol (20 ml). Hydrazine clorhydrate (0.65 g, 9.42 mmol) in water (15 ml) was very slowly added over the solution, and after 4 h the methanol was eliminated at reduced pressure and dichloromethane was added as extracting solvent. The extracts were dried overnight on sodium sulphate, and then filtered. The solvent was removed in vacuo.

Compound **2** resulted as solid, and compound **1** appeared as an oil which was transformed to solid after several hours. Yields are given in Table 1.

2.2. Preparation of [Rh(Cl)(Hpz^R)(LL)] (LL = NBD, COD; R = pp, bp) (3–6)

To a yellow solution of [Rh(μ-Cl)(LL)]$_2$ (LL = NBD, COD) (0.2 mmol) in dichloromethane (15 ml) was added the corresponding pyrazole (0.4 mmol). The clear yellow solution that formed immediately after the addition was stirred at room temperature for 2 h. Then the vol-ume was reduced in vacuo to approximately 2 ml. Addition of hexane caused the precipitation of a yellow solid, which was filtered off, washed with small portions of hexane and dried in vacuo. Yields are given in Table 2.

2.3. Preparation of [Rh(Cl)(Hpz^R)(CO)$_2$] (R = pp, bp) (7,8)

Carbon monoxide was bubbled about ca. 20 min through a solution of [Rh(Cl)(Hpz^R)(LL)] (LL = NBD, COD; R = pp, bp) in dichloromethane (20 ml) at room

Table 1
IR data, isolated yield, melting point and elemental analyses of Hpz^{pp} (1) and Hpz^{bp} (2)

	IR ^{a} (cm^{-1})		Yield (%)	M.p. (°C)	Molecular formula	Calculated (%)			Found (%)		
	ν(NH)	ν(CN)				C	H	N	C	H	N
1	3200	1590	35	95	$C_{15}H_{12}N_2O$	76.24	5.13	11.86	75.63	5.31	12.07
2	3190–3142	1612	40	60–62	$C_{13}H_{16}N_2O$	72.18	7.47	12.95	72.11	7.38	12.68

^{a} In KBr discs.

Table 2
IR data, colour, isolated yield and elemental analyses of complexes [Rh(Cl)(Hpz^R)(LL)] (LL = NBD, COD, 2CO; R = pp, bp) (3–8)

	IR ^{a} (cm^{-1})				Colour	Yield (%)	Molecular formula	Calculated (%)			Found (%)		
	ν(NH)	ν(CN)	β(CH)	ν(CO)				C	H	N	C	H	N
3	3232	1589	1305		yellow	79	$C_{22}H_{20}N_2OClRh$	56.60	4.33	6.00	55.94	4.29	5.93
4	3250	1590	1300		yellow	87	$C_{23}H_{24}N_2OClRh$	57.21	5.02	5.80	56.86	4.85	5.66
5	3304	1614	1306		yellow	85	$C_{20}H_{24}N_2OClRh$	53.75	5.38	6.27	53.38	5.23	6.24
6	3224	1616	1305		yellow	91	$C_{21}H_{28}N_2OClRh$	54.49	6.05	6.05	54.33	5.76	5.88
7	3287	1589		2089	blue-violet	72	$C_{17}H_{12}N_2O_3ClRh$	47.41	2.81	6.51	48.12	2.80	6.23
				2057									
				2013									
				1995									
8	3300	1614		2083	violet	74	$C_{15}H_{16}N_2O_3ClRh$	43.85	3.90	6.82	44.08	3.98	6.60
				2058									
				2004									
				1996									

^{a} In KBr discs.

Table 3
IR data, colour, isolated yield and elemental analyses of complexes [Rh(μ-pz^R)(LL)]$_2$ (LL = NBD, COD, 2CO; R = pp, bp) (9–14)

	IR ^{a} (cm^{-1})			Colour	Yield (%)	Molecular formula	Calculated (%)			Found (%)		
	ν(CN)	β(CH)	ν(CO)				C	H	N	C	H	N
9	1590	1302		orange-red	70	$C_{44}H_{38}N_4O_2Rh_2$	61.40	4.46	6.51	60.82	4.35	6.74
10	1589	1300		deep-yellow	77	$C_{46}H_{46}N_4O_2Rh_2$	61.62	5.10	6.25	61.88	5.20	6.28
11	1612	1295		orange-red	72	$C_{40}H_{46}N_4O_2Rh_2$	58.53	5.84	6.81	58.87	5.38	6.53
12	1612	1300		deep-yellow	81	$C_{42}H_{54}N_4O_2Rh_2$	59.03	6.56	6.56	59.01	6.30	6.49
13	1592		2089	yellow	62	$C_{34}H_{22}N_4O_6Rh_2$	51.79	2.82	7.11	51.50	2.61	6.95
			2075									
			2018									
14	1611		2096	yellow	74	$C_{30}H_{30}N_4O_6Rh_2$	48.01	4.27	7.47	48.69	4.26	7.19
			2072									
			2039									
			2003									

^{a} In KBr discs.

temperature and atmospheric pressure. The initial yellow colour of the solution changed to lighter yellow. The blue-violet residue obtained by evaporation was recrystallized by dissolving it in dichloromethane and adding diethyl ether. The blue-violet solid obtained was filtered off and dried in vacuo. Yields are given in Table 2.

2.4. Preparation of [Rh(μ-pz^R)(LL)]$_2$ (LL = NBD, COD, R = pp, bp) (9–12)

To a suspension of [Rh(μ-Cl)(LL)]$_2$ (LL = NBD, COD) (0.2 mmol) in methanol (15 ml) was added the corresponding pyrazole Hpz^R (R = pp, bp) (0.4 mmol). To the clear yellow solution immediately formed was added a solution of KOH in methanol (5 ml) in aliquots of 1 ml during a period of 30 s, and a yellow-orange solid precipitated. The mixture was stirred for 15 min and then the solid was filtered off, washed with cold methanol and hexane and dried in vacuo. Yields are given in Table 3.

2.5. Preparation of [Rh(μ-pz^R)(CO)$_2$]$_2$ (R = pp, bp) (13,14)

Carbon monoxide was bubbled about ca. 45 min through a solution of [Rh(μ-pz^R)(LL)]$_2$ (LL = NBD,

COD; R = pp, bp) in dichloromethane (20 ml) at room temperature and atmospheric pressure. The initial yellow-orange colour of the solution changed to light yellow. The yellow residue obtained by evaporation was treated with diethyl ether and evaporated again to dryness. The yellow solid was washed with cold hexane and dried in vacuo. Yields are given in Table 3.

2.6. X-ray structure determination

Colourless prismatic single crystals of Hpz^{pp} (1) were obtained from dichloromethane–diethyl ether and yellow-orange prismatic crystals of [Rh(μ-pz^{pp})(COD)]$_2$ · ½CH$_2$Cl$_2$ (10) and [Rh(μ-pz^{bp})(COD)]$_2$ (12) were obtained from dichloromethane–hexane.

The data were collected on an Enraf–Nonius CAD4 diffractometer for the three compounds, and unit cell constants were refined from least squares fitting of the θ values of 25 reflections with 2θ of 12–24° for 1, 15–29° for 10 and 13–27° for 12. A summary of the fundamental crystal data for the three crystals is given in Table 4, and the final values of all refined atomic coordinates are given in Tables 5–7.

The intensities were corrected for Lorentz and polarization effects. Scattering factors for neutral atoms and anomalous dispersion corrections for Rh and Cl atoms

Table 4
Crystal and refinement data for Hpz^{pp} (1), [Rh(μ-pz^{pp})(COD)]$_2$ · ½CH$_2$Cl$_2$ (10) and [Rh(μ-pz^{bp})(COD)]$_2$ (12)

	(1)	(10)	(12)
Formulae	[N$_2$C$_{15}$OH$_{12}$]$_2$	[RhN$_2$C$_{23}$OH$_{23}$]$_2$ · ½CH$_2$Cl$_2$	[RhN$_2$C$_{21}$OH$_{27}$]$_2$
Mr	472.545	935.173	852.726
Crystal system	monoclinic	monoclinic	monoclinic
Space group	$P2_1/n$	$C2/c$	$C2/c$
a (Å)	18.991(3)	12.660(5)	19.703(3)
b (Å)	5.743(2)	37.944(6)	8.835(5)
c (Å)	23.810(7)	17.915(2)	24.478(5)
β (deg)	111.95(2)	107.90(2)	114.48(3)
V (Å^3)	2409(1)	8189(4)	3877(2)
Z	4	8	4
F(000)	992	3816	1760
ρ(calcd) (g cm^{-3})	1.30	1.52	1.46
Temp. (K)	295	295	295
μ (cm^{-1})	0.78	9.0	8.8
Cryst. dimens. (mm)	0.25 × 0.3 × 0.25	0.2 × 0.15 × 0.15	0.15 × 0.15 × 0.15
Diffractometer	Enraf–Nonius CAD4	Enraf–Nonius CAD4	Enraf–Nonius CAD4
Radiation	graphite-monochromated	graphite-monochromated	graphite-monochromated
	Mo Kα (λ = 0.71069 Å)	Mo Kα (λ = 0.71069 Å)	Mo Kα (λ = 0.71069 Å)
Scan technique	ω–2θ	ω–2θ	ω–2θ
Data collected	(−25, 0, 0) to (25, 7, 31)	(−15, 0, 0) to (15, 45, 21)	(−25, 0, 0) to (23, 10, 29)
θ	1 < θ < 28	1 < θ < 25	1 < θ < 25
Unique data	5813	7197	3411
Unique data (*I*) ≥ 2σ(*I*)	1666	3151	2675
R(int) (%)	0.9	1.1	3.3
Std. rflns.	3/222	3/158	2/104
R$_F$ (%)	4.8	6.0	2.9
Rw$_F$ (%)	4.6	6.3	3.1
Average shift/error	0.12	0.51	0.04

Table 5
Atomic coordinates and thermal parameters for Hpz^{pp} (1)

Atom	x	y	z	U_{eq} [a]
N11	−0.2552(3)	−0.8152(12)	0.1999(3)	47(3)
N12	−0.2091(3)	−0.6258(12)	0.2151(3)	44(3)
C13	−0.1954(4)	−0.5774(14)	0.1650(3)	38(3)
C14	−0.2337(5)	−0.7338(16)	0.1191(4)	53(4)
C15	−0.2705(5)	−0.8843(17)	0.1424(4)	54(4)
C16	−0.1447(4)	−0.3846(14)	0.1642(3)	40(3)
C17	−0.1111(4)	−0.2391(15)	0.2139(3)	49(3)
C18	−0.0615(5)	−0.0646(17)	0.2128(4)	54(4)
C19	−0.0451(5)	−0.031(16)	0.1616(4)	54(4)
C110	−0.0790(5)	−0.1709(18)	0.1119(4)	58(4)
C111	−0.1274(4)	−0.3487(15)	0.1131(4)	48(4)
C112	0.0665(5)	0.1883(17)	0.2085(4)	54(4)
C113	0.1252(5)	0.0310(18)	0.2257(4)	63(4)
C114	0.1911(6)	0.0830(23)	0.2742(5)	75(5)
C115	0.1976(6)	0.2893(22)	0.3040(5)	74(5)
C116	0.1383(7)	0.4414(21)	0.2860(5)	83(6)
C117	0.0731(6)	0.3964(17)	0.2376(5)	71(5)
O1	0.0020(3)	0.1467(11)	0.1571(3)	78(3)
N21	0.4450(4)	0.4381(15)	0.9308(4)	66(4)
N22	0.5050(4)	0.2920(13)	0.9574(3)	57(3)
C23	0.5040(4)	0.1417(15)	0.9142(4)	46(3)
C24	0.4433(5)	0.1938(17)	0.8602(4)	58(4)
C25	0.4077(5)	0.3810(17)	0.8728(4)	62(4)
C26	0.5622(4)	−0.0414(15)	0.9268(4)	44(3)
C27	0.6228(5)	−0.0470(17)	0.9811(4)	61(4)
C28	0.6778(6)	−0.2177(17)	0.9941(5)	67(4)
C29	0.6712(5)	−0.3886(16)	0.9525(4)	53(4)
C210	0.6116(5)	−0.3909(17)	0.8984(4)	57(4)
C211	0.5570(5)	−0.2183(17)	0.8860(4)	57(4)
C212	0.7881(4)	−0.5404(16)	0.9527(3)	49(4)
C213	0.8015(5)	−0.3497(17)	0.9241(4)	59(4)
C214	0.8673(6)	−0.3400(22)	0.9117(5)	78(5)
C215	0.9167(7)	−0.5174(25)	0.9261(5)	95(6)
C216	0.9037(6)	−0.7100(23)	0.9554(5)	95(6)
C217	0.8392(6)	−0.7210(19)	0.9688(4)	68(5)
O2	0.7246(3)	−0.5679(11)	0.9669(3)	68(3)

[a] $U_{eq} = 1/3\Sigma_i\Sigma_j U_{ij} a_i^* a_j^* \boldsymbol{a}_i \cdot \boldsymbol{a}_j \times 10^3$.

were taken from the *International Tables for X-ray Crystallography* [8].

The structures were solved by Patterson and Fourier methods. Empirical absorption corrections [9] were applied at the end of the isotropic refinements. The maximum and minimum absorption correction factors were 1.178 and 0.548 for **1**, 1.188 and 0.743 for **10** and 1.157 and 0.804 for **12**.

Final mixed refinements with unit weights were performed for the three compounds with the following differences. For **1**, the hydrogen atoms were located in a difference synthesis and their coordinates refined. In the case of **10** and **12**, the hydrogen atoms were situated in fixed geometrically calculated positions. The solvent molecule in **10** was refined only isotropically. These

Table 6
Atomic coordinates and thermal parameters for [Rh(μ-pz^{pp})(COD)]$_2$ · $\frac{1}{2}$CH$_2$Cl$_2$ (10)

Atom	x	y	z	U_{eq} [a]
Rh1	0.8717(1)	0.15010(3)	0.2470(1)	429(5)
Rh2	0.8711(1)	0.08040(3)	0.7443(1)	384(5)
C11	0.8799(14)	0.1890(5)	0.3316(11)	524(71)
C12	0.7930(16)	0.1675(5)	0.3295(11)	610(81)
C13	0.6692(15)	0.1776(6)	0.2866(12)	662(83)
C14	0.6349(15)	0.1698(7)	0.2062(14)	815(105)
C15	0.7226(18)	0.1664(5)	0.1651(12)	654(86)
C16	0.8018(17)	0.1920(5)	0.1669(12)	650(86)
C17	0.8140(18)	0.2273(5)	0.2117(11)	666(84)
C18	0.8712(17)	0.2257(6)	0.2971(12)	710(91)
N21	1.0872(10)	0.1196(3)	0.3366(7)	400(49)
N22	0.9778(10)	0.1163(4)	0.3284(8)	451(54)
C23	0.9645(14)	0.0910(4)	0.3761(10)	439(64)
C24	1.0689(15)	0.0773(5)	0.4179(10)	531(72)
C25	1.1425(14)	0.0963(5)	0.3896(10)	554(71)
C26	0.8565(14)	0.0782(4)	0.3771(9)	436(64)
C27	0.7650(13)	0.0782(5)	0.3087(9)	467(62)
C28	0.6681(13)	0.0663(5)	0.3143(9)	461(63)
C29	0.6466(14)	0.0540(5)	0.3780(11)	534(73)
C210	0.7341(14)	0.0527(5)	0.4454(11)	537(74)
C211	0.8370(16)	0.0657(5)	0.4459(10)	515(73)
C212	0.4950(13)	0.0561(5)	0.4285(11)	514(72)
C213	0.5125(15)	0.0903(5)	0.4554(12)	602(83)
C214	0.4617(15)	0.1027(6)	0.5062(12)	654(86)
C215	0.3902(17)	0.0816(7)	0.5293(11)	704(91)
C216	0.3727(16)	0.0482(6)	0.5048(12)	655(88)
C217	0.4239(14)	0.0346(5)	0.4529(11)	603(73)
O1	0.5406(10)	0.0412(4)	0.3749(7)	708(57)
C31	0.8823(16)	0.0424(5)	0.8330(9)	559(74)
C32	0.7886(14)	0.0624(5)	0.8241(9)	466(67)
C33	0.6757(17)	0.0496(6)	0.7855(15)	902(110)
C34	0.6312(15)	0.0599(6)	0.6963(11)	672(87)
C35	0.7246(13)	0.0608(5)	0.6612(10)	490(69)
C36	0.8100(12)	0.0362(5)	0.6712(9)	452(59)
C37	0.8060(17)	0.0026(5)	0.7156(15)	830(105)
C38	0.8870(19)	0.0053(5)	0.8009(12)	801(94)
N41	1.0837(11)	0.1090(3)	0.8400(7)	434(53)
N42	0.9737(10)	0.1141(3)	0.8274(7)	372(48)
C43	0.9615(14)	0.1357(5)	0.8832(10)	458(66)
C44	1.0641(14)	0.1442(5)	0.9335(10)	516(68)
C45	1.1408(14)	0.1276(4)	0.9045(9)	443(65)
C46	0.8510(13)	0.1485(4)	0.8834(9)	370(58)
C47	0.7680(17)	0.1550(5)	0.8127(11)	638(82)
C48	0.6617(15)	0.1682(5)	0.8066(11)	648(80)
C49	0.6443(14)	0.1758(5)	0.8798(12)	542(80)
C410	0.7250(14)	0.1699(5)	0.9485(10)	486(69)
C411	0.8278(14)	0.1569(4)	0.9503(10)	471(71)
C412	0.5155(19)	0.2055(6)	0.9327(12)	663(97)
C413	0.5746(19)	0.2333(6)	0.9692(13)	737(99)
C414	0.5358(25)	0.2502(8)	1.0247(16)	1036(140)
C415	0.4356(28)	0.2399(9)	1.0349(18)	1219(159)
C416	0.3802(26)	0.2133(9)	0.9959(18)	1149(158)
C417	0.4161(19)	0.1950(6)	0.9444(15)	825(114)
O2	0.5402(11)	0.1871(4)	0.8726(8)	889(70)
C1	0.5000(0)	0.3023(10)	0.2500(0)	1379(116)
Cl	0.3728(6)	0.2826(2)	0.2074(4)	1646(22)

[a] $U_{eq} = 1/3\Sigma_i\Sigma_j U_{ij} a_i^* a_j^* \boldsymbol{a}_i \cdot \boldsymbol{a}_j \times 10^4$.

Table 7

Atomic coordinates and thermal parameters for [Rh(μ-pz^{bp})(COD)]$_2$ (12)

Atom	x	y	z	U_{eq} [a]
Rh	0.58992(2)	0.02955(4)	0.27509(1)	410(1)
C1	0.61012(26)	−0.13242(50)	0.34330(19)	558(20)
C2	0.67296(24)	−0.04420(55)	0.35908(18)	573(18)
C3	0.7437(28)	−0.09600(68)	0.35428(25)	791(25)
C4	0.74427(28)	−0.05303(74)	0.29467(28)	894(29)
C5	0.66790(29)	−0.04744(65)	0.24385(23)	707(24)
C6	0.61411(31)	−0.15653(63)	0.23148(22)	711(25)
C7	0.62407(35)	−0.30415(62)	0.26598(27)	867(30)
C8	0.60126(32)	−0.29039(56)	0.31742(26)	776(27)
N11	0.46889(17)	0.14663(38)	0.30316(14)	449(13)
N12	0.54211(17)	0.17369(36)	0.31686(14)	410(13)
C13	0.56828(21)	0.27129(45)	0.36305(17)	432(16)
C14	0.51143(25)	0.30700(58)	0.37992(21)	642(22)
C15	0.45049(23)	0.22645(57)	0.34120(20)	585(20)
C16	0.64434(21)	0.33326(43)	0.38634(17)	420(16)
C17	0.68370(23)	0.34276(48)	0.35087(18)	488(17)
C18	0.75223(24)	0.41074(53)	0.37146(19)	540(19)
C19	0.78273(22)	0.47501(53)	0.42808(19)	537(17)
C110	0.74572(25)	0.46507(59)	0.46470(19)	616(19)
C111	0.67664(24)	0.39436(53)	0.44331(19)	545(18)
C112	0.88549(28)	0.61201(65)	0.50035(22)	735(23)
C113	0.95251(28)	0.69611(63)	0.50242(23)	726(24)
C114	1.00064(32)	0.75119(79)	0.56204(26)	951(31)
C115	1.06960(29)	0.83422(69)	0.56674(26)	847(27)
O1	0.84936(17)	0.54816(41)	0.44229(14)	711(15)

$U_{eq} = 1/3 \Sigma_i \Sigma_j U_{ij} a_i^* a_j^* \boldsymbol{a}_i \cdot \boldsymbol{a}_j \times 10^4$.

refinements led to the R values given in Table 4. None of the three final difference syntheses showed significant electron density. No trend in ΔF vs. F_o or $(\sin \theta)/\lambda$ were observed.

Most of the calculations were carried out with the X-RAY 80 program [10]. Full lists of atomic coordinates, thermal parameters and bond lengths and angles have been deposited at the Cambridge Crystallographic Data Centre.
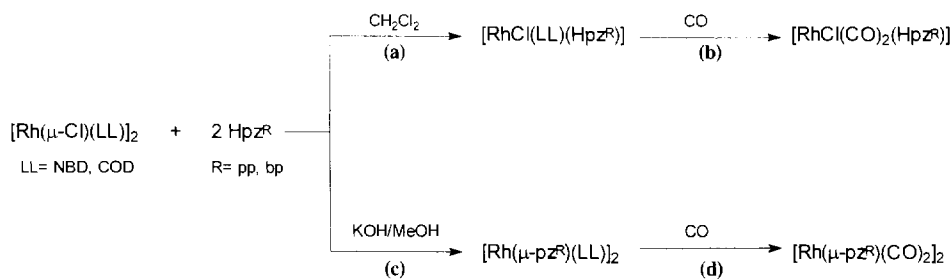
3. Results and discussion

3.1. Compounds Hpz^{pp} (1) and Hpz^{bp} (2)

The compounds 1,2 were prepared by analogous procedures that those described for Hpz$^{3(5)R}$ ligands [11–13]. The physical properties, IR data and elemental analyses are given in Table 1.

The ^{1}H and ^{13}C NMR data are recovered in Tables 8 and 9. Assignment of the signals was made following the literature precedents [14–16].

In agreement with related aryl-substituted pyrazoles, two tautomeric forms, Hpz^{3R} or Hpz^{5R}, or a tautomeric equilibrium could be expected for these heterocycles [14]. From our NMR data, we can deduce the presence of only one tautomer or a very fast equilibrium between

Table 8

^{1}H NMR data of pyrazoles 1 and 2 in CDCl$_3$ (300.13 MHz) at 298 K

	Pyrazole			−C$_6$H$_4$−		−OR′
	NH	H$_4$	H$_5$	H$_o$	H$_m$	
1	11.6br s	6.61d $J_{45} = 2.2$	7.67d	7.72d $J_{om} = 8.3$	7.03d	H$_{o'}$: 7.06d H$_{m'}$: 7.37t H$_{p'}$: 7.14t $J_{o'm'} = J_{m'p'} = 8.3$
2	12.71br s	6.51d $J_{45} = 2.2$	7.57d	7.65d $J_{om} = 8.5$	6.90d	CH$_2$-1′: 3.97t $J_{1'2'} = 6.6$ CH$_2$-2′: 1.78q $J_{2'3'} = 7.7$ CH$_2$-3′: 1.51st $J_{3'4'} = 7.1$ CH$_3$-4′: 0.99t

br s = broad signal, d = doublet, t = triplet, q = quintuplet, st = sextuplet.

Table 9

^{13}C{^{1}H} NMR data of pyrazoles 1 and 2 in CDCl$_3$ (75.43 MHz) at 298 K

	Pyrazole carbons			−C$_6$H$_4$−				−OR′
	C$_3$	C$_4$	C$_5$	C$_\alpha$	C$_o$	C$_m$	C$_p$	
1	148.5br s	102.3	132.9br s	130.2	129.7	119.0 [a]	157.1 [b]	C$_{\alpha'}$: 156.8 [b] C$_{o'}$: 118.9 [a] C$_{m'}$: 127.3 C$_{p'}$: 123.4
2	148.3br s	101.8	133.8br s	124.4	127.0	114.6	159.0	C1′: 67.6 C2′: 31.2 C3′: 19.2 C4′: 13.8

br s = broad signal.

[a,b] The assignment could also be the opposite one.

the two tautomeric forms on the NMR time scale at room temperature.

As was described for the related 3(5)-phenylpyrazole, the major tautomer found in solution was the 3-one which was also the structure of the solid [14]. The crystal structure of **1**, as will be described below, indicates the presence of the 3-tautomer in the solid.

On the above basis, we can suggest for **1** and **2** that the 3-tautomer must be present in both the solution and the solid state.

3.1.1. Crystal structure of 1

An X-ray study of the compound Hpz^{pp} has been carried out. Table 10 lists the selected bond lengths, bond angles and dihedral angles.

There are two independent dimeric entities, labelled as A and B, in the asymmetric unit, with slight differences in the dihedral angles (Table 10). No interaction between them is observed.

Each dimeric entity is formed by two symmetrically related molecules through hydrogen bonds (Fig. 1).

As in other pyrazoles [14,18], compound **1** shows the characteristic bond distances of a delocalized ring. The main bond angles, C(5)–N(1)–N(2) and C(3)–N(2)–N(1), of 112.3(7), 104.4(7)° and 110.9(8), 105.7(7)° for A and B dimers respectively (Table 10), follow the same sequence as in other pyrazoles with the H(1)

Fig. 1. Perspective ORTEP [17] of Hpz^{pp}, **1**, (molecule A) with atomic numbering scheme. The hydrogen atoms (except those corresponding to the hydrogen bond) have been omitted for clarity.

proton localized [14,19,20]. The other angles within the pyrazole rings are close, being larger at C(3) probably due to the presence of the substituent in this position.

Table 10
Selected bond distances (Å), angles (deg) and angles (deg) between the least squares sets defined by the specified atoms for Hpz^{pp} (**1**) with ESDs in parenthesis

Molecule A		Molecule B	
N11–N12	1.36(1)	N21–N22	1.36(1)
N11–C15	1.35(1)	N21–C25	1.34(1)
N12–C13	1.34(1)	N22–C23	1.34(1)
C13–C14	1.39(1)	C23–C24	1.40(1)
C13–C16	1.47(1)	C23–C26	1.47(1)
C14–C15	1.35(1)	C24–C25	1.36(1)
N11–H11	0.97(9)	N21–H21	0.85(9)
N12'...H11	2.01(9)	N22"...H21	2.14(9)
N12–N11–C15	112.3(7)	N22–N21–C25	110.9(8)
N11–N12–C13	104.4(7)	N21–N22–C23	105.7(7)
N12–C13–C16	120.8(7)	N22–C23–C26	120.7(8)
N12–C13–C14	110.3(8)	N22–C23–C24	109.8(8)
C14–C13–C16	128.9(8)	C24–C23–C26	129.5(8)
C13–C14–C15	106.8(8)	C23–C24–C25	105.8(9)
N11–C15–C14	106.3(8)	N21–C25–C24	107.8(9)
H11–N11–N12	120(5)	H21–N21–N22	107(6)
N11–H11–N12'	167(8)	N21–H21–N22"	153(7)
1 - N11,N12,C13,C14,C15		1 - N21,N22,C23,C24,C25	
2 - C16,C17,C18,C19,C110,C111		2 - C26,C27,C28,C29,C210,C211	
3 - C112,C113,C114,C115,C116,C117		3 - C212,C213,C214,C215,C216,C217	
1–2	4.3(3)		8.3(4)
1–3	91.9(3)		98.8(4)
2–3	87.6(3)		90.5(3)

Symmetry codes :(') $-1/2 - x$, $-1/2 + y$, $1/2 - z$; (") $1 - x$, $1 - y$, $2 - z$.

$$[Rh(\mu\text{-Cl})(LL)]_2 + 2\ Hpz^R \xrightarrow[\qquad]{}$$

- (a) $\xrightarrow{CH_2Cl_2}$ $[RhCl(LL)(Hpz^R)]$ $\xrightarrow[\ (b)\ ]{CO}$ $[RhCl(CO)_2(Hpz^R)]$
- (c) $\xrightarrow{KOH/MeOH}$ $[Rh(\mu\text{-}pz^R)(LL)]_2$ $\xrightarrow[\ (d)\ ]{CO}$ $[Rh(\mu\text{-}pz^R)(CO)_2]_2$

LL = NBD, COD   R = pp, bp

Scheme 2.

3.2. Compounds [Rh(Cl)(Hpz^R)(LL)] (LL = NBD, COD, 2CO; R = pp, bp) (3–8)

Reactions of the dimers $[Rh(\mu\text{-Cl})(LL)]_2$ (LL = NBD, COD) with Hpz^R (R = pp, bp) were performed in dichloromethane in a 1:2 molar ratio (Scheme 2(a)). All the isolated complexes are yellow air-stable solids characterized as $[Rh(Cl)(Hpz^R)(LL)]$ (LL = NBD, COD; R = pp, bp) (3–6) by analytical and spectroscopic (IR and ^1H NMR) techniques (Tables 2 and 11).

Table 11

^1H NMR data of compounds $[Rh(Cl)(Hpz^R)(LL)]$ (LL = NBD, COD, 2CO; R = pp, bp) (3–8) in CDCl$_3$ at 298 K

	Pyrazole			$-C_6H_4-$		$-OR'$	LL
	NH	H4	H5 [a]	H$_o$	H$_m$		
3	12.18br	6.43d $J_{45}=2.1$	6.77d	7.47d $J_{om}=8.8$	7.03d	H$_{o'}$: 7.04d H$_{m'}$: 7.37t H$_{p'}$: 7.16t $J_{o'm'}=J_{m'p'}=8.3$	CH$_2$-7: 1.33 CH-2,3,5,6: 4.06br s CH-1,4: 3.87
4	12.60br	6.48d $J_{45}=2.2$	7.08d	7.49d $J_{om}=8.5$	7.04d	H$_{o'}$: 7.04d H$_{m'}$: 7.37t H$_{p'}$: 7.16t $J_{o'mp'}=J_{m'p'}=8.5$	CH$_2$-3,4,7,8: 2.50, 1.87d CH-1,2,5,6: 4.43br s
5	12.10br	6.39d $J_{45}=2.1$	6.75d	7.42d $J_{om}=8.7$	6.92d	CH$_2$-1': 3.98t $J_{1'2'}=6.9$ CH$_2$-2': 1.77q $J_{2'3'}=7.8$ CH$_2$-3': 1.49st $J_{3'4'}=7.5$ CH$_3$-4': 0.98t	CH$_2$-7: 1.33 CH-2,3,5,6: 4.06br s CH-1,4: 3.86
6	12.50br	6.44d $J_{45}=2.1$	7.06d	7.45d $J_{om}=8.7$	6.93d	CH$_2$-1': 3.98t $J_{1'2'}=6.6$ CH$_2$-2': 1.78q $J_{2'3'}=7.8$ CH$_2$-3': 1.50st $J_{3'4'}=7.2$ CH$_3$-4': 0.98t	CH$_2$-3,4,7,8: 2.50, 1.87d CH-1,2,5,6: 4.04br s
7	11.60br	6.60br	7.63br	7.52d $J_{om}=8.3$	7.07m	H$_{o'}$: 7.07m H$_{m'}$: 7.38t H$_{p'}$: 7.20t $J_{p'm'}=J_{m'p'}=8.3$	
8	12.20br	6.56br	7.61br	7.48d $J_{om}=8.4$	6.97d	CH$_2$-1': 4.00t $J_{1'2'}=6.6$ CH$_2$-2': 1.79q $J_{2'3'}=7.8$ CH$_2$-3': 1.51st $J_{3'4'}=7.2$ CH$_3$-4': 0.98t	

br s = broad signal, d = doublet, t = triplet, q = quintuplet, st = sextuplet, m = multiplet.

[a] The H5 assignment corresponds to the closest proton to the rhodium atom.

Table 12

$\nu(CO)$ bands of $[Rh(Cl)(CO)_2(Hpz^R)]$ (R = pp, bp) (7,8) in different solvents [a]

	$[Rh(Cl)(CO)_2(Hpz^{pp})]$ (7)				$[Rh(Cl)(CO)_2(Hpz^{bp})]$ (8)			
Solid state (KBr)	2089	2013	2057	1995	2083	2004	2058	1996sh
Dichloromethane	2089	2016			2089	2017	2058sh	2004sh
Carbon tetrachloride	2089	2013	2059sh	1993sh	2087	2013	2058sh	2000sh
Hexane	2086	2010	2079sh	2023sh	2087	2011	2058sh	2004sh
Acetonitrile	2067	1990			2067	1990		
Acetone	2061	1982	2077sh	2017sh	2060	1982	2085sh	2002m
Ethanol	2075	1996	2090m	2022m	2069	1996	2077m	2002m

[a] sh = shoulder, m = medium. Other bands are very strong.

Bubbling CO through a dichloromethane solution of [Rh(Cl)(Hpz^R)(LL)] (LL = NBD, COD; R = pp, bp) gave rise to the dicarbonyl complexes [Rh(Cl)(CO)$_2$(Hpz^R)] (R = pp, bp) (**7,8**) (Scheme 2(b)) as blue-violet solids but yellow in solution (Tables 2, 11 and 12). This behaviour is characteristic of the presence of metal–metal interactions in the solid, as had already been observed in related compounds [3,21]. These complexes are slightly unstable in solution and evolve after several hours.

The ^{1}H NMR spectra at room temperature of **3–8** (Table 11), related to the coordinated pyrazol ligand, consist of two signals corresponding to the H(4) and H(5) protons, which are broad when LL is 2CO (**7,8**). This fact is attributed to the presence of a metallotropic equilibrium as represented in Fig. 2, which does not take place for the COD and NBD derivatives (**3–6**) or it is very fast on the NMR time scale. Then the exchange rate between the two metallotropic forms (I and II) seems to depend on the ancillary ligands present in the complexes, and the increase of the steric requirements in the order COD > NBD > 2CO appears to avoid the metallotropic exchange.

However, by contrast, it is remarkable that the olefinic complexes **3–6** present broad signals corresponding to the olefinic protons, H2, H3, H5 and H6 for derivatives
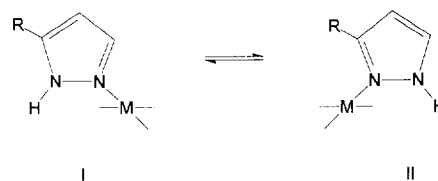
Fig. 2.

3 and 5, and H1, H2, H5 and H6 for derivatives **4** and **6** (Scheme 1, Table 11). This fact is attributed to a reorientation of the coordinated diene, as had already been observed in related Rh(I) complexes [3,5].

The IR spectra in the solid state of the derivatives [Rh(Cl)(CO)$_2$(Hpz^R)] (**7,8**) (R = pp, bp) in the carbonyl region show two split ν(CO) absorptions of similar intensity. However, only two strong bands with two weak shoulders are observed in solution for most of the solvents (Table 12). This result is consistent with the presence in solution of the two metallotropic forms (I and II), and is in agreement with a metallotropic equilibrium already proposed by ^{1}H NMR (Fig. 2). By considering the intensity of the ν(CO) bands in solution, the equilibrium should be displaced towards one of the two isomeric forms (probably that with the sub-

Table 13
^{1}H NMR data of compounds [Rh(μ-pz^R)(LL)]$_2$ (LL = NBD, COD, 2CO; R = pp, bp) (**9–14**) in CDCl$_3$ (300.13 MHz) at 298 K

	Pyrazole		$-C_6H_4-$		$-OR'$	LL
	H4	H5	H$_o$	H$_m$		
9	6.21	7.22	8.31br	7.16d	H$_{o'}$: 7.16d	CH$_2$-7: 1.45–1.20
			J_{om} = 8.2		H$_{m'}$: 7.36t	CH-2,3,5,6: 4.29–3.32
					H$_{p'}$: 7.11t $J_{o'm'} = J_{m'p'}$ = 7.7	CH-1,4: 4.29–3.32
10	6.21d	7.42d	8.24d	7.13d	H$_{o'}$: 7.13d	CH$_2$-3,4,7,8: 3.00–2.60, 2.10–1.60
	J_{45} = 1.8		J_{om} = 8.5		H$_{m'}$: 7.36t	CH-1,2,5,6: 4.61, 4.10, 3.48
					H$_{p'}$: 7.07t $J_{o'm'} = J_{m'p'}$ = 7.7	
11	6.17	7.20d	8.25br	7.07d	CH$_2$-1': 4.09t $J_{1'2'}$ = 6.3	CH$_2$-7: 1.43–1.11
	J_{45} = 2.2		J_{om} = 7.1		CH$_2$-2': 1.81q $J_{2'3'}$ = 7.2	CH-2,3,5,6: 4.27–3.28
					CH$_2$-3': 1.53m $J_{3'4'}$ = 7.2	CH-1,4: 4.27–3.28
					CH$_3$-4': 1.04t	
12	6.16d	7.42d	8.16d	6.99d	CH$_2$-1': 4.03t $J_{1'2'}$ = 6.3	CH$_2$-3,4,7,8: 2.90–2.65, 2.20–1.80
	J_{45} = 1.8		J_{om} = 8.7		CH$_2$-2': 1.82q $J_{2'3'}$ = 7.8	CH-1,2,5,6: 4.60, 4.07, 3.45
					CH$_2$-3': 1.52st $J_{3'4'}$ = 7.2	
					CH$_3$-4': 1.00t	
13	6.46d	7.65d	7.88d	7.10m	H$_{o'}$: 7.10m	
	J_{45} = 1.7	7.61d [a]	J_{om} = 8.3		H$_{m'}$: 7.38t, 7.35t [a]	
	6.47d [a]		7.91d [a]		H$_{p'}$: 7.10m $J_{o'm'} = J_{m'p'}$ = 7.2, 7.7 [a]	
	J_{45} = 2.2		J_{om} = 8.3			
14	6.43	7.65	7.81d	6.89d	CH$_2$-1': 4.03t, 4.05t [a] $J_{1'2'}$6.6	
		7.59 [a]	J_{om} = 8.3	7.01d [a]	CH$_2$-2': 1.83q $J_{2'3'}$ = 7.8	
			7.88d [a]		CH$_2$-3': 1.52st $J_{3'4'}$ = 7.2	
			J_{om} = 8.3		CH$_3$-4': 1.00t, 1.02t [a]	

br s = broad signal, d = doublet, t = triplet, q = quintuplet, st = sextuplet, m = multiplet.
[a] Minor isomer (ratio of isomers is ca. 60/40).

stituent in the 3-position on the pyrazol ring, I), and only in ethanol is the second isomer clearly observed. It is interesting to note that solvents with higher coordinating ability, like ethanol, acetone or acetonitrile, give rise to lower ν(CO) frequency values. Therefore, this behaviour is attributed to the interaction of the complex with the solvent.

3.3. Complexes [Rh(μ-pz^R)(LL)]$_2$ (LL = COD, NBD, 2CO; R = pp, bp) (9–14)

Reaction of chloro-bridged dimers [Rh(μ-Cl)(LL)]$_2$ (LL = COD, NBD) with a stoichiometric amount of Hpz^R (R = pp, bp) in methanol and addition of KOH–MeOH led to dinuclear complexes [Rh(μ-pz^R)(LL)]$_2$ (9–12) (LL = NBD, COD; R = pp, bp) as air-stable yellow-orange solids (Scheme 2(c)).

The carbonyl derivatives [Rh(μ-pz^R)(CO)$_2$]$_2$ (13,14) (R = pp, bp) were obtained by reaction of [Rh(μ-pz^R)(LL)]$_2$ (LL = NBD, COD; R = pp, bp) and CO in dichloromethane (Scheme 2(d)). The isolated complexes are yellow solids and their purity has been ascertained by elemental analyses.

The synthetic procedures are analogous to that previously used for related compounds [4,22,23]. Complexes 9–14 have been characterized by analytical and spectroscopic techniques (Tables 3, 13 and 14).

As has been described in previous work [4,24], owing to the unsymmetrical substitution of the bridging ligands, the dinuclear compounds can exist as two configurational isomers, containing the two pyrazol-bridges oriented H-H having a C_s symmetry and H-T having a C_2 symmetry, as depicted in Fig. 3.

Our previous results in related dimers complexes [Rh(μ-pz^{3R,5R})(NBD)]$_2$ established that the steric hindrance of the substituents on the pyrazol ring could be responsible for the formation of only one isomer or a mixture of them. So, with 3-t-butylpyrazol or 5-methyl-3-t-butylpyrazol ligands the isomers H-H or H-T were respectively isolated, but pyrazolate-ligands containing aryl substituents like pz^{Ph}, pz^{An}, pz^{Me,Ph} gave rise to a mixture of both isomers [4].

Surprisingly, in this work, when we use 1 and 2, one almost pure isomer (the ratio of isomers is ca. 10/1) is produced when COD or NBD are the ancillary ligands present (9–12). However, the related dicarbonyl deriva-

Table 14
^{13}C{^{1}H} NMR data of complexes [Rh(μ-pz^R)(LL)]$_2$ (LL = NBD, COD, 2CO; R = pp, bp) (9–14) in CDCl$_3$ (75.43 MHz) at 298 K

	pz			–C$_6$H$_4$–				–OR'	LL
	C$_3$	C$_4$	C$_5$	C$_\alpha$	C$_o$	C$_m$	C$_p$		
9	150.6	103.5	138.3	130.0	129.8	118.8 [a]	157.5 [b]	C$_{\alpha'}$: 156.2 [b] C$_{o'}$: 118.6 [a] C$_{m'}$: 128.4 C$_{p'}$: 123.0	CH$_2$-7: 62.04 CH-2,3,5,6: 55.7–59.2 CH-1,4: 51.5–50.0
10	150.9	103.4	137.8	130.3	129.7	118.8 [a]	157.7 [b]	C$_{\alpha'}$: 156.1 [b] C$_{o'}$: 118.4 [a] C$_{m'}$: 128.6 C$_{p'}$: 123.0	CH$_2$-3,4,7,8: 32.0, 31.9, 30.9, 29.4 CH-1,2,5,6: 83.0d, 82.2d, 81.6d, 77.3d J_{Rh} = 11–13
11	151.0	103.2	138.1	127.2	128.1	114.1	158.4	CH$_2$-1': 67.8 CH$_2$-2': 31.5 CH$_2$-3': 19.3 CH$_3$-4': 13.9	CH$_2$-7: 62.0 CH-2,3,5,6: 59.0–57.3 CH-1,4: 51.4–50.5
12	151.2	103.0	137.6	127.5	129.4	113.9	158.3	CH$_2$-1': 67.8 CH$_2$-2': 31.4 CH$_2$-3': 19.2 CH$_3$-4': 13.9	CH$_2$-3,4,7,8: 32.0, 31.9, 30.8, 29.4 CH-1,2,5,6: 82.8d, 82.0d, 81.5d, 77.1d J_{Rh} = 11–13
13	153.9	104.7 105.1 [c]	142.7 143.3 [c]	128.7	129.8	118.5 [a]	157.6 [b]	C$_{\alpha'}$: 156.9 [b] C$_{o'}$: 119.2 [a], 119.0 [a,c] C$_{m'}$: 129.7, 129.6 [c] C$_{p'}$: 123.5, 123.6 [c]	CO: 185.3 J_{Rh} = 66.8 184.1 [c] J_{Rh} = 65.2
14	154.0	104.4 104.8 [c]	142.6 143.2 [c]	126.2	129.4 129.6 [c]	114.2 114.3 [c]	159.3	CH$_2$-1': 67.4, 67.8 [c] CH$_2$-2': 31.3, 31.4 [c] CH$_2$-3': 19.3 CH$_3$-4': 13.9	CO: 185.5 J_{Rh} = 67.1 184.1 [c] J_{Rh} = 72.5

[a,b] The assignment could also be the opposite one.
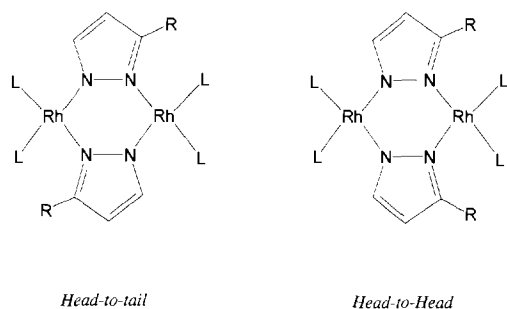[c] Minor isomer (ratio of isomers is ca. 60/40).

Head-to-tail   Head-to-Head

Fig. 3. H-H and H-T configurational isomers of [Rh(μ-pz^R)(LL)]$_2$.

tives (13,14) have been obtained as a mixture of both isomers.

The ^{1}H and ^{13}C NMR spectra of derivatives 9–12 (Tables 13 and 14) agree with the presence of a major isomer. The ratio of the two isomers has been deduced by integration of the C_o and C_m carbons of the C_6H_4 group and a value of ca. 10/1 has been found for all the complexes. The assignments of the signals have been performed following the previous criteria established for the ligands and for related complexes [14–16].

It is interesting to note that the resonances of the *ortho* protons of the C_6H_4 group of the substituent on the pyrazol ring are more shifted towards lower field with respect to the free pyrazole ligand than the other aromatic resonances (Table 13). The values of these H-*ortho* chemical shifts indicate a considerable deshielding consistent with a possible hydrogen–rhodium interaction.

Furthermore, in these complexes the two *ortho* protons on the mentioned C_6H_4 group give rise to only one signal which is broad for NBD derivatives (9,11) but well-resolved for COD derivatives (10,12). Thus, it must induce that the rotation of the C_6H_4 group of the substituent is fast on the NMR time scale, but it is faster for the COD-derivatives (10,12) than for the NBD-ones (9,11).

For these compounds 9–12 one finds, by ^{1}H and ^{13}C

NMR spectroscopies, only one type of the C_6H_4 group and the expected olefinic resonances for only one configurational isomer. So, the diolefinic moiety gives rise to six (four CH-olefinic and two CH-tertiary) signals for NBD derivatives and four CH-olefinic signals for COD derivatives. These results are consistent with an H-T configuration in both cases, but an H-H configuration could not be excluded in the case of COD derivatives for which the same number of signals is expected.

Then, the crystalline structures of 10 and 12 have been solved in order to confirm the above proposal for the solids. From these X-ray structures, as will be described below, the H-T configurational isomer is evidenced for both dimers, in which the central Rh(NN)$_2$Rh ring exists in a boat conformation. From the above results, we suggest the presence of the same configurational isomer in solution.

In principle the NMR results of 10 and 12 suggest a static conformation of the boat Rh(NN)$_2$Rh, probably favoured for the presence of COD as ancillary ligand and by the Rh–H interaction with the C_6H_4 group on the pyrazol ring.

The same behaviour could be suggested for 9 and 11, although in these cases motions of the diolefinic ligands should not be excluded, due to the slight broadness of the NBD signals. From the position of the *ortho* protons of the C_6H_4 groups on the pyrazol ring, the H–Rh interaction could be considered stronger for the NBD-derivatives (9,11) than that proposed for the COD-ones (10,12). This fact is in agreement with the suggested slower mobility of the C_6H_4 group in 9 and 11 than in 10 and 12.

The presence of an Rh–H interaction, albeit of a weak type, might make a contribution to the lack of the inversion of the boat-like Rh(NN)$_2$Rh ring, which, however, has been observed in related complexes [25,26].

The ^{1}H and ^{13}C NMR spectra of carbonyl derivatives (13,14) are in agreement with a mixture of isomers, the ratio of H-T/H-H being 60/40, determined by ^{1}H NMR spectroscopy by integration of the resonances of
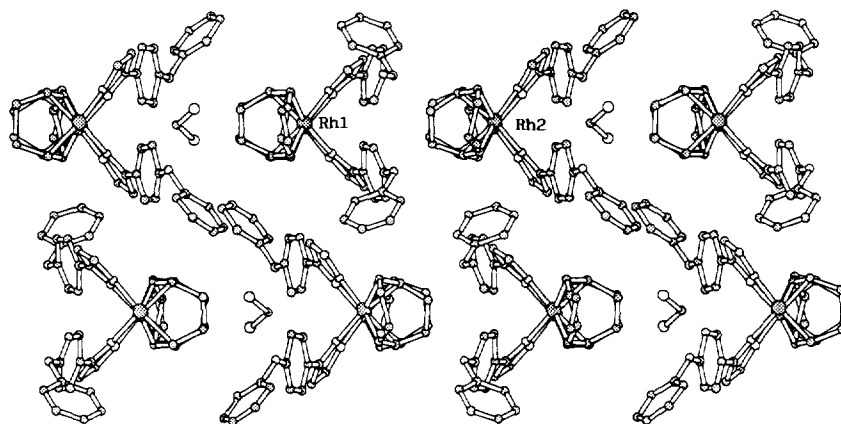

Fig. 4. Packing arrangement of [Rh(μ-pz^{PP})(COD)]$_2$ · $\frac{1}{2}$CH$_2$Cl$_2$ (10) viewed down the a axis.

the *ortho* protons of the C_6H_4 group, which is resolved into two doublets at room temperature (Table 13).

In addition, the ^{13}C NMR spectra clearly show two signals for all the carbons, and the ratio of isomers (60/40) is also confirmed by integration of the C_4 resonances of the pyrazol ring (Table 14).

3.3.1. X-ray crystal structures of [Rh(μ-pz^{PP})(COD)]₂ · ½CH₂Cl₂ (10) and [Rh(μ-pz^{bp})(COD)]₂ (12)

The X-ray structure of Rh(μ-pz^{PP})(COD)]₂ · ½CH₂Cl₂ (10) and [Rh(μ-pz^{bp})(COD)]₂ (12) confirms the dimeric neutral nature of both compounds. The complexes are formed by two rhodium atoms, two pyrazolate rings bridging the two metals and two olefinic groups. Each rhodium atom in both compounds exhibits a square-plane coordination, and the two rhodium and the four nitrogen atoms of the two bridged pyrazolate rings give rise to a metallocycle ring $Rh(NN)_2Rh$ in a boat conformation. The substituents on the pyrazol ring are situated in an H-T position.

Some crystallographic differences are observed between both structures. So, compound 10 crystallizes with a half molecule of dichloromethane (Fig. 4) and its structure shows the existence of two different crystallographic molecules, labelled A and B respectively (Figs. 5 and 6). By contrast, complex 12 does not present crystallization molecules in its structure, in which there is only an independent crystallographic molecule (Fig. 7).

However, most of the structural features are similar in both compounds. The complexes crystallize in the $C2/c$ space group, and both contain a twofold axis which passes through the middle of a hypothetical line between the two rhodium atoms. Tables 15 and 16 show selected bond distances and angles in both compounds.

Considering the least-square plane formed by the four nitrogen atoms of the pyrazol-bridged rings in the metallocycle $Rh(NN)_2Rh$, the distances from the rhodium atom to this plane are 1.220(1) Å and 1.197(1) Å for molecules A and B respectively of 10, being longer than the 1.160(2) Å observed for 12. The dihedral angles between the plane formed by the four

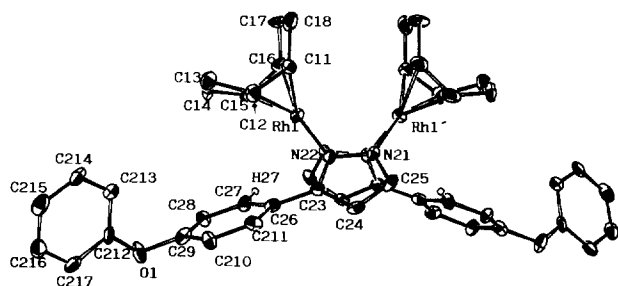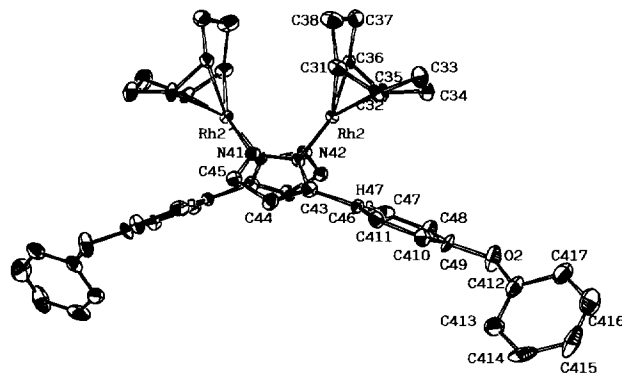Fig. 6. Perspective ORTEP [17] of [Rh(μ-pz^{PP})(COD)]₂ · ½CH₂Cl₂, 10, (molecule B). The solvent and the hydrogen atoms have been omitted for clarity.

nitrogen atoms and the NRhN planes are 52.7(7)° and 52.5(6)° in molecules A and B of 10 and 50.7(2)° for 12. These facts are in agreement with the Rh1–Rh2 distances found of 3.219(3) Å, 3.208(3) Å for molecules A and B respectively of 10 and 3.2339(9) Å in 12.

These rhodium–rhodium distances are significatively shorter than 3.267(2) Å found in [Rh(μ-pz)(COD)]₂ [27] as consequence of the substitution on the pyrazol ring, but longer than that observed in related complexes containing bulky substituted pyrazol and NBD as ancillary ligand [4].

The orthogonal orientation of the COD ligand in both complexes is deduced from the values of dihedral angles between planes 2–3, which were 91.8(7)° (A), 90.0(6)° (B) in 10 and 90.5(2)° in 12 (Table 17).

The dihedral angle between the planes 4–2 (Table 17), of 70.1(6)° and 68.4(5)° in A and B of 10, and 70.4(2)° in 12, reveals that the bridged pyrazol lies in a position intermediate between normal and parallel.

All the above structural features are analogous to that observed in related H-T compounds [4].

However, the orientation of the C_6H_4 group of the substituent on the pyrazol ring in both compounds merits further comments. The values of dihedral angles between the C_6H_4 and pyrazol planes (planes 4–5) of
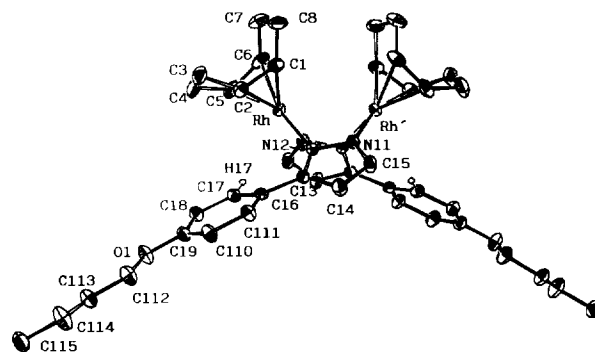

Fig. 5. Perspective ORTEP [17] of [Rh(μ-pz^{PP})(COD)]₂ · ½CH₂Cl₂, 10, (molecule A). The solvent and the hydrogen atoms have been omitted for clarity.

Fig. 7. Perspective ORTEP [17] of [Rh(μ-pz^{bp})(COD)]₂, 12. The hydrogen atoms have been omitted for clarity.

Table 15

Selected bond distances (Å) and angles (deg) for [Rh(μ-pz^{pp})(COD)]$_2$ · $\frac{1}{2}$CH$_2$Cl$_2$ (10) with ESDs in parentheses

Molecule A		Molecule B	
Rh1–Rh1′	3.219(3)	Rh2–Rh2″	3.208(3)
Rh1–C11	2.10(2)	Rh2–C31	2.12(2)
Rh1–C12	2.13(2)	Rh2–C32	2.13(2)
Rh1–C15	2.10(2)	Rh2–C35	2.12(1)
Rh1–C16	2.14(2)	Rh2–C36	2.12(2)
Rh1–N22	2.09(1)	Rh2–N42	2.09(1)
Rh1–N21′	2.08(1)	Rh2–N41″	2.08(2)
Rh1–C1112	2.00(2)	Rh2–C3132	2.01(2)
Rh1–C1516	2.00(2)	Rh2–C3536	2.00(2)
N22–N21	1.35(2)	N42–N41	1.35(2)
N22–C23	1.33(2)	N42–C43	1.34(2)
N21–C25	1.33(2)	N41–C45	1.36(2)
C25–C24	1.39(3)	C45–C44	1.39(3)
C24–C23	1.40(2)	C44–C43	1.37(2)
Rh1…H27	2.734(2)	Rh2…H47	2.879(1)
N22–Rh1–N21′	85.0(5)	N42–Rh2–N41′	87.1(6)
C1516–Rh1–N21′	93.2(7)	C3536–Rh2–N41″	94.3(6)
C1516–Rh1–N22	175.5(7)	C3536–Rh2–N42	177.6(6)
C1112–Rh1–N21′	177.7(7)	C3132–Rh2–N41″	177.1(7)
C1112–Rh1–N22	92.8(7)	C3132–Rh2–N42	91.3(6)
C1112–Rh1–C1516	89.1(8)	C3536–Rh2–C3132	87.4(7)

Symmetry codes: (′) 2 − x, y, 1/2 − z; (″) 2 − x, y, 3/2 − z.

34.2(7)° and 33.5(8)° for A and B of **10** (Table 17) are modified with respect to those observed in the free ligand (4.3(3)° and 8.3(4)° for A and B units of **1**, Table 4). This situation gives rise to a proximity of the protons in *ortho* position of the C$_6$H$_4$ group to the rhodium centres, which also should occur in **12**. So, the

Table 16

Selected bond distances (Å) and angles (deg) for [Rh(μ-pz^{bp})(COD)]$_2$ (12) with ESDs in parentheses

Rh–Rh′	3.2339(9)
Rh–C1	2.1075(5)
Rh–C2	2.131(4)
Rh–C5	2.094(7)
Rh–C6	2.119(6)
Rh–N12	2.087(4)
Rh–N11′	2.059(3)
Rh–C1122	2.005(4)
Rh–C5566	1.993(7)
N11–N12	1.360(5)
N11–C15	1.332(7)
N12–C13	1.344(5)
C13–C14	1.381(8)
C14–C15	1.379(6)
Rh…C17	3.4164(4)
Rh…H17	2.7007(1)
N12–Rh–N11′	87.4(1)
C5566–Rh–N11′	93.5(2)
C5566–Rh–N12	176.7(2)
C1122–Rh–N11′	176.7(2)
C1122–Rh–N12	91.2(2)
C1122–Rh–C5566	88.1(2)

Symmetry code: (′) 1 − x, y, 1/2 − z.

Table 17

Selected angles (deg) between the least squares sets defined by the specified atoms for [Rh(μ-pz^{pp})(COD)]$_2$ · $\frac{1}{2}$ (10) and [Rh(μ-pz^{bp})(COD)]$_2$ (12)

(10) molecule A		
1 – N21,N22,N21′,N22′	1–2	51.4(6)
2 – N21′,N22,C1112,C1516	1–3	40.5(8)
3 – C11,C12,C15,C16	2–3	91.8(7)
4 – N21,N22,C23,C24,C25	1–4	46.5(8)
5 – C26,C27,C28,C29,C210,C211	4–7	86.5(6)
6 – C212,C213,C214,C215,C216	4–5	34.2(7)
7 – N21′,N22′,C23′,C24′,C25′	4–6	62.1(6)
	5–6	73.0(6)
(10) molecule B		
1 – N41,N42,N41″,N42″	1–2	52.4(6)
2 – N41″,N42,C3132,C3536	1–3	38.0(8)
3 – C31,C32,C35,C36	2–3	90.1(6)
4 – N41,N42,C43,C44,C45	1–4	37.4(6)
5 – C46,C47,C48,C49,C410,C211	4–7	74.8(7)
6 – C412,C413,C414,C415,C416	4–5	33.5(8)
7 – N41″,N42″,C43″,C44″,C45″	4–6	32.8(6)
	5–6	60.7(7)
(12)		
1 – N11,N12,N11‴,N12‴	1–2	50.8(2)
2 – N11‴,N12,C1122,C5566	1–3	39.1(2)
3 – C1,C2,C5,C6	2–3	90.5(2)
4 – N11,N12,C13,C14,C15	1–4	39.8(1)
5 – C16,C17,C18,C19,C110,C111	4–7	79.5(1)
7 – N11‴,N12‴,C13‴,C14‴,C15‴	4–5	25.4(2)

C1112, C1516, C3132 and C3536 are the midpoints of (C11,C12), (C15,C16), (C31,C32) and (C35,C36) respectively for (10). C1122 and C5566 are the midpoints of (C1,C2) and (C5,C6) respectively for (12).

Symmetry codes (10): (′) 2 − x, y, 1/2 − z; (″) 2 − x, y, 3/2 − z; Symmetry code (12): (‴) 1 − x, y, 1/2 − z.

Rh–H distances were 2.734(2) Å and 2.879(1) Å for A and B in **10** and 2.7007(1) Å for **12**. Although these distances are longer than typical separations of the agostic type, which are in the range of 1.8–2.2 Å [26], they are shorter than the sum of the van der Waals radii of the rhodium and hydrogen atoms and suggest an interaction although weak.

An Rh–H interaction, described as of preagostic type, has been found in [Rh(C_8H_{14})B(pz)$_2$}(COD)] as responsible for a square-pyramidal coordination on the rhodium atom, being in this case the Rh–H distance of 2.42 Å [26]. In our complexes the Rh–H distance of ca. 2.7 Å agrees with the presence of a weak preagostic interaction of the type of that reported previously [28–31].

4. Supplementary material available

Tables giving fractional coordinates and thermal parameters, bond distances and angles, and observed and calculated structure factors for **1** (3, 7 and 39 pages respectively), **10** (5, 13 and 48 pages respectively) and **12** (3, 7 and 23 pages respectively) can be obtained from the authors.

Acknowledgements

References

[1] S. Trofimenko, Prog. Inorg. Chem., 34 (1986) 115.

[2] H. Schumann, H. Hemling, V. Ravinder, Y. Badrieh and J. Blum, J. Organomet. Chem., 469 (1994) 213, and references cited therein.

[3] M. Cano, J.A. Campo, J.V. Heras, J. Lafuente, C. Rivas and E. Pinilla, Polyhedron, 14 (1995) 1139.

[4] C. López, J.A. Jiménez, R.M. Claramunt, M. Cano, J.V. Heras, J.A. Campo, E. Pinilla and A. Monge, J. Organomet. Chem., 511 (1996) 115.

[5] M. Cocivera, G. Ferguson, F.J. Lalor and P. Szczecinski, Organometallics, 1 (1982) 1139.

[6] E.W. Abet, M.A. Bennett and G. Wilkinson, J. Chem. Soc., (1959) 3178.

[7] J. Chatt and L.M. Venanzi, J. Chem. Soc., (1957) 4735.

[8] International Tables for X-ray Crystallography, Vol. 4, Kynoch, Birmingham, 1974, pp. 72–98.

[9] N. Walker and D. Stuart, Acta Crystallogr. Sect. A:, 39 (1983) 158.

[10] J.M. Stewart, The X-ray 80 System, 1985 (Computer Science Center, University of Maryland, College Park, MD).

[11] S. Trofimenko, J.C. Calabrese, P.J. Domaille and J.S. Thompson, Inorg. Chem., 28 (1989) 1091.

[12] S. Trofimenko, J.C. Calabrese, J.K. Kochi, S. Wolowiec, F.B. Hulsbergen and J. Reedjik, Inorg. Chem., 31 (1992) 3943.

[13] S. Trofimenko, J.C. Calabrese and J.S. Thompson, Inorg. Chem., 26 (1987) 1507.

[14] F. Aguilar-Parrilla, C. Cativiela, M.D. Díaz de Villegas, J. Elguero, C. Foces-Foces, J.I. García-Laureiro, F. Hernández-Cano, H.H. Limbach, J.A.S. Smith and C. Toiron, J. Chem. Soc. Perkin Trans. 2:, (1992) 1737.

[15] M. Begtrup, G. Boyer, P. Cabildo, C. Cativiela, R.M. Claramunt, J. Elguero, J.I. García, C. Toiron and P. Vedsø, Magn. Reson. Chem., 31 (1993) 107.

[16] C. López, D. Sanz, R.M. Claramunt, S. Trofimenko and J. Elguero, J. Organomet. Chem., 503 (1995) 265.

[17] C.K. Johnson, ORTEP, Rep. ORNL-3794, 1971 (Oak Ridge National Laboratory, Oak Ridge, TN).

[18] E.N. Maslen, J.R. Cannon, A.H. White and A.C. Willis, J. Chem. Soc. Perkin Trans. 2:, (1975) 1068.

[19] F.H. Allen, O. Kennard and R. Taylor, Acc. Chem. Res., 16 (1983) 146.

[20] J.A.S. Smith, B. Wehrle, F. Aguilar-Parrilla, H.H. Limbach, C. Foces-Foces, F.H. Cano, J. Elguero, A. Baldy, M. Pierrot, M.M.T. Khurshid and J.R. Larcombe-McDowall, J. Am. Chem. Soc., 111 (1989) 7304.

[21] M.J. Decker, D.O. Kimberley Fjeldsted, S.R. Stobart and M.J. Zaworotko, J. Chem. Soc. Chem. Commun., (1983) 1525.

[22] R. Usón, M.A. Ciriano, M.T. Pinillos, A. Tiripicchio and M. Tiripicchio Camellini, J. Organomet. Chem., 205 (1981) 247.

[23] R. Usón, L.A. Oro, M.A. Ciriano and M.C. Bello, J. Organomet. Chem., 240 (1982) 199.

[24] F. Bonati, L.A. Oro, M.T. Pinillos, C. Tejel and B. Bovio, J. Organomet. Chem., 465 (1994) 267.

[25] M.A. Ciriano, M.A. Tena and L.A. Oro, J. Chem. Soc. Dalton Trans., (1992) 2123.

[26] M. Bortolin, U.E. Bucher, H. Rüegger, L.M. Venanzi, A. Albinati, F. Lianza and S. Trofimenko, Organometallics, 11 (1992) 2514.

[27] K.A. Beveridge, G.W. Bushnell, S.R. Stobart, J.L. Atwood and M.J. Zaworotko, Organometallics, 2 (1983) 1447.

[28] A. Albinati, P.S. Pregosin and F. Wombacher, Inorg. Chem., 29 (1990) 1812.

[29] C.G. Anklin and P.S. Pregosin, Magn. Reson. Chem., 23 (1985) 671.

[30] A. Albinati, C.G. Anklin, F. Ganazzoli, H. Rüegg and P.S. Pregosin, Inorg. Chem., 26 (1987) 503.

[31] A. Albinati, C. Arz and P.S. Pregosin, Inorg. Chem., 26 (1987) 508.